Ocean acidification of the Greater Caribbean Region 1996–2006

Dwight K. Gledhill,[1] Rik Wanninkhof,[2] Frank J. Millero,[3] and Mark Eakin[1]

Received 9 November 2007; revised 5 May 2008; accepted 20 August 2008; published 31 October 2008.

[1] The global oceans serve as the largest sustained natural sink for increasing atmospheric carbon dioxide (CO_2) concentrations. As this CO_2 is absorbed by seawater, it not only reacts causing a reduction in seawater pH (or acidification) but also decreases the carbonate mineral saturation state (Ω), which plays an important role in calcification for many marine organisms. Ocean acidification could affect some of the most fundamental biological and geochemical processes of the sea in coming decades. Observations obtained *in situ* from Volunteer Observing Ships and multiple geochemical surveys have been extended using satellite remote sensing and modeled environmental parameters to derive estimates of sea-surface alkalinity (A_T) and carbon dioxide partial pressure ($pCO_{2,sw}$). Pairing estimates of A_T and $pCO_{2,sw}$ have permitted characterization of the changes in sea-surface Ω, which have transpired over the past decade throughout the Greater Caribbean Region as a consequence of ocean acidification. The results reveal considerable spatial and temporal variability throughout the region. Despite this variability, we observed a strong secular decrease in aragonite saturation state (Ω_{arg}) at a rate of approximately $-0.012 \pm 0.001\ \Omega_{arg}\ yr^{-1}$ ($r^2 = 0.97$, $P < 0.001$).

Citation: Gledhill, D. K., R. Wanninkhof, F. J. Millero, and M. Eakin (2008), Ocean acidification of the Greater Caribbean Region 1996–2006, *J. Geophys. Res.*, *113*, C10031, doi:10.1029/2007JC004629.

1. Introduction

[2] Anthropogenic activities during the last century have driven atmospheric carbon dioxide (CO_2) concentrations to levels greater than, and increasing at a rate much faster than, experienced on Earth for at least the last 650,000 years [*Petit et al.*, 1999; *Augustin et al.*, 2004; *Siegenthaler et al.*, 2005]. The global oceans are the largest natural reservoir for this excess CO_2, absorbing approximately one-third of that attributed to anthropogenic activities each year [*Sabine et al.*, 2004]. Consequently, dissolved gaseous CO_2 in the surface ocean will likely double over its pre-industrial value by the middle of this century having important consequences for the marine environment. While the ocean's uptake of CO_2 has alleviated some of the atmospheric burden, the subsequent impact on surface ocean chemistry may represent the most dramatic change in over 20 million years [*Feely et al.*, 2004]. When CO_2 reacts with seawater, a series of equilibrium reactions occur including the production of carbonic acid causing a reduction in seawater pH. While seawater is naturally ''buffered'' against such changes, it does so at the expense of carbonate ions which play an important role in the creation of calcium carbonate shells and skeletons produced by a large number of marine organisms (e.g., corals, marine plankton, coralline algae, and shellfish). Such changes in ocean chemistry in response to increasing levels of atmospheric CO_2 have been recognized for more than three decades [e.g., *Broecker et al.*, 1971; *Bacastow and Keeling*, 1972] and are clearly seen in seawater CO_2 observations obtained from several continuous ocean time-series stations and repeated geochemical surveys. These include, for example: BATS (Bermuda Atlantic Time-series Study) in the NW Atlantic Ocean [e.g., *Bates et al.*, 1996; *Bates*, 2007], station ALOHA (A Long-term Oligotrophic Habitat Assessment) near Hawaii in the North Pacific Ocean [e.g., *Karl et al.*, 2001; *Keeling et al.*, 2004] as well as in the World Ocean Circulation Experiment (WOCE) and Joint Global Ocean Flux Study (JGOFS) [*Sabine et al.*, 2004; *Feely et al.*, 2004]. In coming decades, this process of ''ocean acidification'' could affect some of the most fundamental biological and geochemical processes of the sea [*Caldeira and Wickett*, 2003].

[3] A number of biological systems have now demonstrated a sensitivity to changes in carbonate chemistry from reef-building corals and coralline algae [e.g., *Gattuso et al.*, 1998a; *Marubini et al.*, 2001, 2002; *Reynaud et al.*, 2003; *Marshall and Clode*, 2002; *Ohde and Hossain*, 2004; *Borowitzka*, 1981; *Gao et al.*, 1993; *Langdon et al.*, 2000, 2003; *Langdon and Atkinson*, 2005; *Leclercq et al.*, 2000, 2002; *Yates and Halley*, 2006; *Kuffner et al.*, 2008] to phytoplankton [e.g., *Riebesell et al.*, 2000; *Riebesell*, 2004; *Bijma et al.*, 2002]. The effects of ocean acidification on corals, which produce the calcium carbonate mineral aragonite, appears not to be directly related to changes in pH *per se*, but instead related to corresponding changes in carbonate mineral saturation state (Ω), where Ω can be described as the ratio of the ion concentration product ($[Ca^{2+}][CO_3^{2-}]$) to the stoichiometric solubility product (K^*_{sp}) of the mineral phase of interest (typically aragonite) [*Morse and Berner*, 1972]. A near first-order linear rela-

[1] NOAA NESDIS Coral Reef Watch, Silver Spring, Maryland, USA.
[2] NOAA OAR AOML, Miami, Florida, USA.
[3] Rosenstiel School, University of Miami, Miami, Florida, USA.

0148-0227/08/2007JC004629

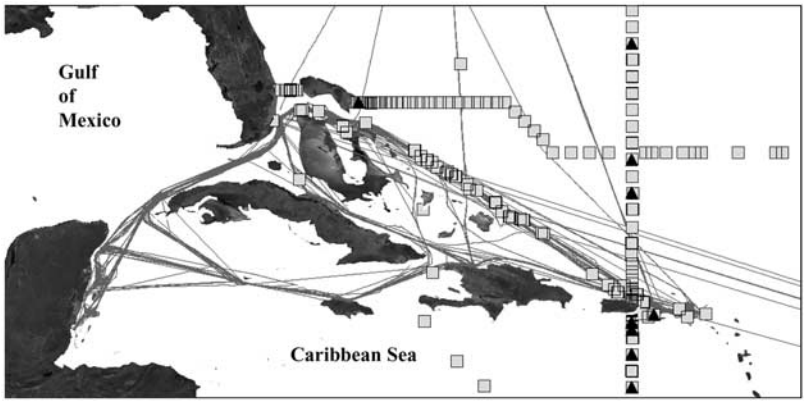

Figure 1. Map of the Greater Caribbean Region. The lines show a composite of the 2002–2006 *Explorer of the Seas* ship tracks where underway $pCO_{2,sw}$ and ancillary data were collected. Discrete measurements of multiple sea-surface carbonate parameters were measured as part of several geochemical surveying efforts throughout the region between 1996 and 2006 (grey squares). These include the ACT Cruises (June 1997), WOCE A22 (August 1997, October 2003), WOCE AR01 (February 1998), selected *Explorer of the Seas* transects (March 2003, May and August 2005, November 2006), and the ABACO Easter Boundary Current Cruise (March 2006). In some instances, only total alkalinity was measured (black triangles).

tionship was observed between calcification rate and aragonite saturation state (Ω_{arg}) by *Langdon and Atkinson* [2005] similar to the inorganic precipitation kinetics described by *Morse et al.* [2003]. Responses beyond the effects on calcification rate have also been observed. For example, a decreased abundance of crustose coralline algae due to ocean acidification has been experimentally demonstrated [*Kuffner et al.*, 2008].

[4] Modern-day ocean carbonate chemistry was computed by *Orr et al.* [2005] from observed total alkalinity (A_T) and dissolved inorganic carbon (DIC) data collected as part of WOCE and JGOFS [*Key et al.*, 2004]. Using these calculations along with simulated DIC from ocean models that were forced by multiple IPCC CO_2 scenarios, they estimated changes in surface Ω_{arg} through the year 2100 [*Orr et al.*, 2005]. Applying the IPCC IS92a "business as usual" scenario, and assuming the calcification rate-Ω_{arg} relationship observed in the experimental studies, they estimated that the resulting changes in surface Ω_{arg} could cause calcification rates to decline by up to 50% by 2100. Such projections have garnered considerable interest from the coral community as this would likely compromise coral reef accretion. These models currently contain important omissions in that they exclude much of the Greater Caribbean Region, Gulf of Mexico, and the "coral triangle" (Indonesian-Philippines Region and Far Southwestern Pacific Region). These are non-trivial omissions as these waters contain vast coral reef ecosystems that may be negatively impacted by ocean acidification. We focus here on estimating the carbonate chemistry changes that have transpired over the past decade in one such region: the Greater Caribbean Region (GCR).

[5] Using the convention employed by *Olsen et al.* [2004], we refer to the GCR as the region comprising waters 90°–60°W, 15°–30°N. This region houses extensive carbonate platform production and coral reef ecosystems including those of the Antilles island arc, Puerto Rico, Hispaniola, Jamaica, Cuba, Bahamas, and the Florida Keys. The waters of this region are predominantly oligotrophic and similar to the subtropical gyre from which it receives most of its water. These reefs are important to the US and many Caribbean nations with an estimated annual net economic value between US$3.1–4.6 billion in 2000 [*Burke and Maidens*, 2004]. Unfortunately, at least 2/3 of Caribbean reefs are threatened by numerous local threats with some of the greatest threats coming from human population growth, overfishing, coastal development, sediments, land-based pollution, nutrient runoff, boat damage and coral disease [*Burke and Maidens*, 2004; *Kleypas and Eakin*, 2006]. Climatic threats of rising ocean temperatures and ocean acidification further exacerbate the problems facing Caribbean reefs.

[6] Here we extend observations obtained *in situ* from the Volunteer Observing Ship *Explorer of the Seas* and multiple geochemical surveys using satellite remote sensing and modeled environmental parameters to estimate the seasonal and spatial variability in Ω_{arg} and to evaluate the changes in surface ocean chemistry that have transpired over the past decade throughout the GCR.

2. Methods and Data

2.1. General Approach

[7] In order to fully describe the carbonic acid system and solve for Ω_{arg}, it is required that at least two of the carbonate parameters ($pCO_{2,sw}$, A_T, DIC, pH) be known. To achieve this, we have computed daily fields of A_T and $pCO_{2,sw}$ (carbon dioxide partial pressure) through the application of a variety of modeled and remotely sensed environmental parameters. Sea-surface $pCO_{2,sw}$ was estimated using an empirical model relating the differential between sea-surface and atmospheric CO_2 partial pressure ($\Delta pCO_2 = pCO_{2,sw} - pCO_{2,air}$) to changes in CO_2 gas solubility (K_0). Sea-surface A_T was derived using the empirical relationships recently offered by *Lee et al.* [2006] describing (sub)tropical

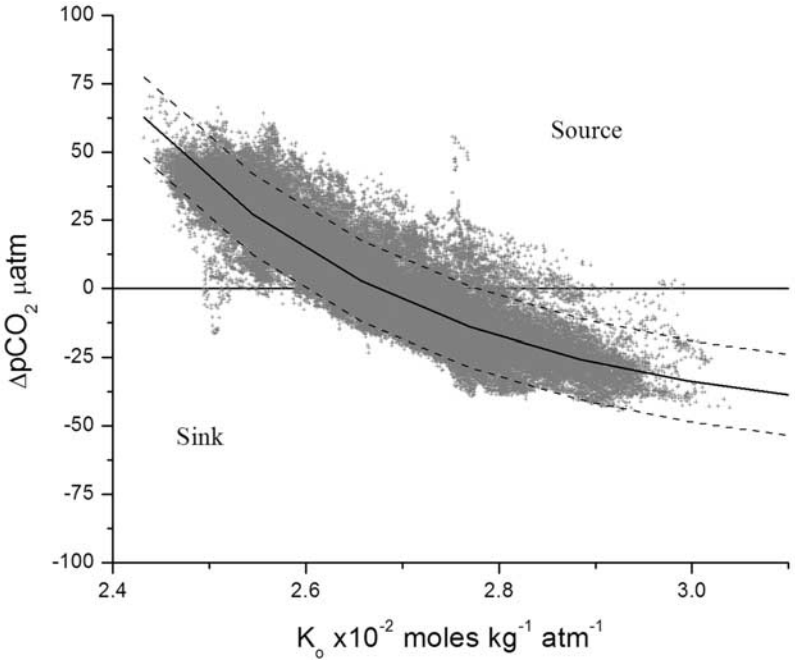

Figure 2. The gas solubility coefficient was calculated for each Explorer of the Seas observation (2002–2006) using the on-board thermosalinograph (TSG) data. Differences between the measured $pCO_{2,sw}$ and atmospheric $pCO_{2,air}$ (ΔpCO_2) are shown as a first-order exponential decay function of increasing gas solubility ($\Delta pCO_2 = y_0 + A_1 EXP(-K_0/t_1)$, $r^2 = 0.85$, 95% prediction bands shown as dashed lines).

surface A_T as a function of sea-surface salinity (SSS) and temperature (SST). Monthly composites of these A_T and $pCO_{2,sw}$ fields were then coupled to solve the carbonic acid system using the CO2SYS program [*Lewis and Wallace*, 1998].

2.2. Computation of Sea-Surface $pCO_{2,sw}$ Fields

[8] Sea-surface $pCO_{2,sw}$ was modeled using an empirical $\Delta pCO_{2,sw}$-K_0 relationship derived using underway $pCO_{2,sw}$, SST, SSS, and sea level barometric pressure (SLP) measurements taken aboard the *Explorer of the Seas*. The ship is operated by Royal Caribbean International and maintained by the University of Miami's Rosenstiel School of Marine and Atmospheric Sciences and the National Oceanic and Atmospheric Administration's (NOAA) Atlantic Oceanographic & Meteorological Laboratory (AOML). Until recently, the vessel has made alternating east and west tracks throughout the GCR and was equipped with an underway $pCO_{2,sw}$ analyzer beginning in February 2002 (Figure 1). The details of this system are provided elsewhere [*Olsen et al.*, 2004; *Feely et al.*, 1998; *Wanninkhof and Thoning*, 1993]. Briefly, the seawater used by the Seabird thermosalinograph and $pCO_{2,sw}$ system is drawn from an intake situated at 2 m depth close to the ship's bow. Headspace from an equilibrator chamber is passed through a LI-COR 6251 nondispersive infrared analyzer and the resulting $pCO_{2,sw}$ value (μatm) is corrected to *in situ* conditions using the iso-chemical temperature dependency of *Takahashi et al.* [1993]. Weekly quality controlled *Explorer of the Seas* data are available from the NOAA AOML Global Carbon Cycle (GCC) Program at http://www.aoml.noaa.gov/ocd/gcc/explorer_introduction.php.

[9] Atmospheric CO_2 partial pressure ($pCO_{2,air}$) was computed according to:

$$pCO_{2,atm} = XCO_2(SLP - pH_2O) \quad (1)$$

where SLP was as measured by the underway barometric pressure system, water vapor pressure (pH_2O) was calculated as a function of thermosalinograph SST (SST_{TSG}) according to the empirical formula offered by *Cooper et al.* [1998], and the dry atmospheric CO_2 mole fraction data (XCO_2) were obtained from the NOAA Global Monitoring Division (GMD) Carbon Cycle Cooperative Global Air Sampling Network [*Thoning et al.*, 1995; http://www.esrl.noaa.gov/gmd/ccgg/index.html]. The XCO_2 flask data 1996–2006 from Key Biscayne, Fl (25.7°N) and Ragged Point, Barbados (13.2°N) were interpolated to derive daily estimates and linearly regressed to account for any latitudinal gradient across the region in the fashion employed by *Olsen et al.* [2004]. Using this approach, a ΔpCO_2 value was obtained for each *Explorer of the Seas* observation as a function of $pCO_{2,sw}$, SLP_{ship}, SST_{TSG} and a date and latitude-dependent XCO_2. The temperature and salinity-dependent gas solubility coefficient (K_0, moles kg^{-1} atm^{-1}) was calculated according to *Weiss* [1974] using the thermosalinograph data.

[10] A common approach to modeling $pCO_{2,sw}$ has been to apply simple multivariate statistical regression analysis relating $pCO_{2,sw}$ to SST, latitude, and longitude [e.g., *Olsen et al.*, 2004; *Wanninkhof et al.*, 2007; *Goyet et al.*, 1998]. Such an approach has proven quite successful at modeling fields of $pCO_{2,sw}$ constrained to the time period from which the *in situ* measurements on which algorithms are based.

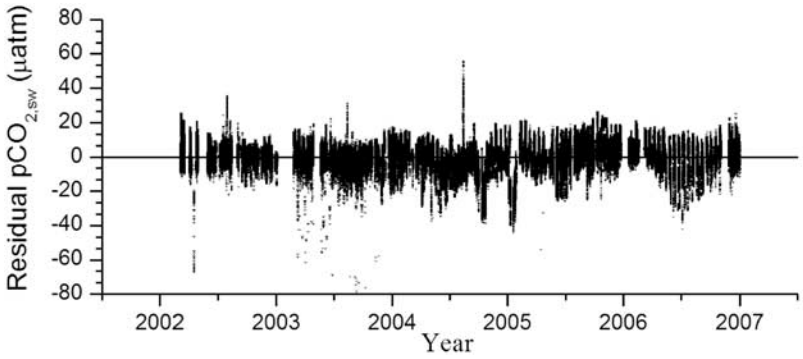

Figure 3. Calculated residuals between $pCO_{2,sw}$ values as computed using equation (3) solved using *Explorer of the Seas* TSG data versus that measured by the underway $pCO_{2,sw}$ analyzer. This single algorithm exhibits no systematic change in the residual distribution over time. The mean and standard deviation of the residuals are 0.40 ± 7.6 μatm (n = 314510).

However, while the primary control on $pCO_{2,sw}$ in these oligotrophic surface waters is thermodynamic (i.e., temperature & salinity), these waters also reflect changes induced as a consequence of the rising atmospheric CO_2 to which they are in contact. Therefore it can be expected that such algorithms become increasingly biased outside the sampling domain requiring an independently derived algorithm specific to each year [*Wanninkhof et al.*, 2007]. In addition, these algorithms provide no mechanistic attribution to the lat/lon dependency. Consequently, we have chosen instead to model the ΔpCO_2 as a function of CO_2 solubility (K_0) thereby accounting for the secular rise in global atmospheric CO_2 and more appropriately attributing the spatial dependence to salinity variations rather than lat/lon. The ΔpCO_2 is shown as a first-order exponential decay function of increasing gas solubility (K_0, 10^{-2} moles kg^{-1} atm^{-1}) according to:

$$\Delta pCO_2 = y_0 + A \times EXP(-K_0/B), r^2 = 0.85,$$
$$\text{RMSD} = 7.18\ \mu\text{atm}, n = 314395 \quad (2)$$

where $y_0 = -51.2 \pm 0.3$, $A = 350.7 \pm 12.3 \times 10^3$, $B = 30.3 \pm 0.1 \times 10^{-2}$ as fit using Origin v6.1 Software [*Yang et al.*, 2003] (Figure 2). Equation (2) can then be rearranged to compute $pCO_{2,sw}$ according to:

$$pCO_{2,sw} = y_0 + A \times EXP(-K_0/B) + pCO_{2,air} \quad (3)$$

[11] This algorithm yields comparable predictive capability to that offered by *Olsen et al.* [2004] exhibiting an r^2 = 0.85 with a root mean square deviation (RMSD) of 7.2 μatm. However, unlike previous algorithms that required unique fitting terms for each year, this approach provides a single equation that captures the secular increase in $pCO_{2,sw}$ and exhibits no systematic change in the residual distribution over time (Figure 3). It also attributes the spatial dependency of the $pCO_{2,sw}$ to thermodynamic variability rather than geographic location. Implicit in equation (3) is that $pCO_{2,sw}$ will increase at the same rate as $pCO_{2,air}$ over time if there are no trends in SST or SSS.

[12] To compute daily fields of $pCO_{2,sw}$, this algorithm was applied to the ¼-degree gridded fields of daily NOAA National Climatic Data Center (NCDC) Optimum Interpolation Advanced Very High Resolution Radiometer (OI-AVHRR) SST, NOAA National Center for Environmental Prediction (NCEP) mean SLP, climatological salinities from the NOAA National Oceanographic Data Center World Ocean Atlas (NODC_WOA94), and interpolated fields of XCO_2 derived from the NOAA GMD Carbon Cycle Cooperative Global Air Sampling Network data at Key Biscayne, FL and Ragged Point, Barbados. The daily ¼-degree gridded NOAA OI-AVHRR SST OI.1 (henceforth referred to as SST_{OI}) blends *in situ* data from ships and buoys with Advanced Very High Resolution Radiometer (AVHRR) infrared satellite SST data and includes a large-scale adjustment of satellite biases with respect to the *in situ* data. The product offers improved spatial and temporal resolution compared with previous weekly 1° OI analyses. The AVHRR blended product uses Pathfinder Version 5 AVHRR data (currently available from January 1985 through December 2005) and operational AVHRR data for 2006 onward. A description of the OI analysis and the daily high-resolution blended product can be found in the study of *Reynolds et al.* [2007] and the data obtained from anonymous ftp at ftp://eclipse.ncdc.noaa.gov. The daily mean SLP data are provided on an approximately 2.5-degree grid from the NOAA Climate Diagnostic Center from anonymous ftp at ftp.cdc.noaa.gov. These were re-gridded using an IDL v6.1 cubic convolution interpolation routine to align with the ¼-degree NOAA SST_{OI}. A similar approach was applied to the monthly 1-degree NODC_WOA94 climatological salinities (henceforth termed SSS_{WOA}) provided by the NOAA/OAR/ESRL PSD, Boulder, Colorado, USA [*Monterey and Levitus*, 1997; http://www.cdc.noaa.gov].

[13] Before computation of the daily $pCO_{2,sw}$ fields, the NOAA SST_{OI} was bias corrected to the ship TSG data. The bias was evaluated by bin-averaging and collocating the *Explorer of the Seas* data at daily ¼-degree resolution. The NOAA SST_{OI} exhibited a systematic negative bias relative to daily bin-averaged SST_{TSG} values (−0.31 ± 0.42°C) and was adjusted using regression analysis according to $SST_{TSG} = 1.70(\pm0.05) + 0.95(\pm0.002)SST_{OI}$, r^2 = 0.93, n = 20814 No correction was applied to the SSS_{WOA} fields which did not

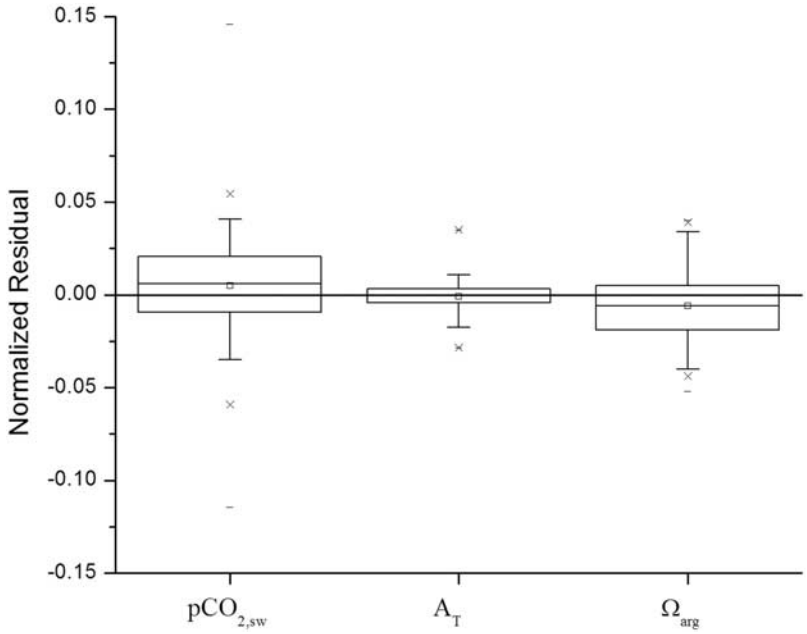

Figure 4. Box plots of the normalized residuals between the calculated fields and bin-averaged collocated geochemical survey data. Residuals, calculated as the difference between the computed fields and collocated ship data, were normalized to the mean ship values. Resolution 0.25° latitude × 0.25° longitude × daily. The line within each box represents the median normalized residual and the center square the mean. Box boundaries indicate 25th (closest to zero) and 75th percentile, and whiskers indicate the 10th and 90th percentiles.

exhibit a systematic bias and showed good agreement with bin-averaged *in situ* data (mean residual = −0.16 ± 0.44 g kg^{-1}, n = 20629).

2.3. Computation of Sea-Surface Total Alkalinity Fields

[14] Estimates of sea-surface total alkalinity (A_T) were derived using the empirical relations offered by *Lee et al.* [2006] for surface waters. *Lee et al.* [2006] demonstrated that about 80% of the variability in surface A_T can be attributed to variations in SSS with a minor dependence on SST. A simple equation of the form:

$$A_T = a + b(SSS - 35) + c(SSS - 35)^2 + d(SST - 20) + e(SST - 20)^2 \quad (4)$$

was derived for each of the five oceanographic regimes. The data used to derive these algorithms were obtained as part of the global inorganic carbon surveys conducted from 1990 to 1998 as part of the Joint Global Ocean Flux Study, the Ocean Atmosphere Carbon Exchange Study, and the World Ocean Circulation Experiment. To compute daily fields of A_T, the (sub)tropical form of the algorithm, which exhibited an area-weighted uncertainty ≥±8.6 μmol kg^{-1} (1σ), was applied to the bias corrected ¼-degree NOAA SST_{OI} and re-gridded SSS_{WOA} fields.

2.4. Computation of Sea-Surface Ω_{arg} Fields

[15] Monthly composites of the daily (1 January 1 1996 to 31 December 2006) $pCO_{2,sw}$, A_T, SST_{OI} and SSS_{WOA} fields were used to solve for the carbon dioxide system parameters and derive estimates of Ω_{arg} throughout the GCR using the CO2SYS program [*Lewis and Wallace*, 1998]. The carbonate equilibria calculations used the formulations by *Mehrbach et al.* [1973] of the K_1 and K_2 dissociation constants as refit by *Dickson and Millero* [1987].

2.5. Evaluation of Computed Fields

[16] Daily computed fields were compared against bin-averaged (¼° × ¼° × daily) geochemical cruise data sets from 1997 through 2006 where sea-surface carbonate chemistry parameters were measured (Figure 1). For $pCO_{2,sw}$ this included all the *Explorer of the Seas* data sets. Cases where at least two carbonate chemistry parameters were measured permitting derivation of Ω_{arg} included the ACT Cruises (June 1997), WOCE A22 (August 1997, October 2003), WOCE AR01 (February 1998; also referred to as WOCE/WHP_A05_1998), selected *Explorer of the Seas* transects (March 2003; May and August 2005; November 2006), and the ABACO Easter Boundary Current Cruise (March 2006) for which the data are made available at http://www.aoml.noaa.gov/ocd/gcc. Residuals were calculated as the difference between the computed $pCO_{2,sw}$, A_T, and Ω_{arg} values and the bin-averaged ship values. In the case of deriving Ω_{arg} ship values, the preferred coupling was A_T and $pCO_{2,sw}$ (n = 61). In cases where $pCO_{2,sw}$ was not measured, A_T and DIC were coupled (n = 38) and in cases where A_T was not measured, $pCO_{2,sw}$ was instead coupled with DIC (n = 15).

[17] The relevant statistics of the residuals are listed in Table 1 and box plots are shown in Figure 4. The normalized residuals were derived by dividing the absolute residual by the mean ship values observed across the entire period (1997–2006). The computed $pCO_{2,sw}$ values show a positive bias of 1.8 ± 8.8 μatm representing less than 0.5 ± 2%.

Table 1. Summary of the Statistics of the Residuals Between Computed $pCO_{2,sw}$, A_T, and Ω_{arg} Fields and Bin-Averaged (0.25° × 0.25° × Daily) Collocated Geochemical Cruise Data

Field	$Mean_{residual}$	$Median_{residual}$	$S.D._{residual}$	$Min_{residual}$	$Max_{residual}$	n	$Mean_{ship}$	$Mean_{model}$
$pCO_{2,sw}$ (μatm)	1.8	2.3	8.8	−43	55	20141	372 ± 18	374 ± 15
A_T (μmol kg^{-1})	−1.9	−0.93	18	−58	72	98	2366 ± 77	2375 ± 36
Ω_{arg}	−0.02	−0.03	0.08	−0.21	0.16	113	4.01 ± 0.17	4.00 ± 0.10

[a]Provided are the descriptive statistics of the residuals, the number of collocations (N), and the mean ± S.D. of ship ($Mean_{obs}$) and modeled ($Mean_{model}$) collocated values. The geochemical survey data represent observations made from 1997 through 2006.

[18] Of the total survey data applied in the derivation by *Lee et al.* [2006] of the (sub)tropical A_T algorithm, samples collected within the marginal basin and coastal regions that constitute the GCR represent only a minor fraction. Despite this, even applied to climatological salinity, the algorithm appears to provide a reasonable estimate of surface A_T in the GCR. The computed A_T values show only a 2 ± 18 μmol kg^{-1} negative bias representing less than 0.1 ± 1%.

[19] The computed Ω_{arg} values exhibit a negative bias of −0.02 ± 0.08, or about 0.5 ± 2%. This is not unreasonable as a 2% precision in Ω_{arg} is within the reported precision of the dissociation constants used by the CO2SYS program. For example, *Mehrbach et al.* [1973] K_1 and K_2 2σ precision is about 2.5% in K_1 and 4.5% in K_2 [*Lewis and Wallace*, 1998]. Also, it is important to consider that the ship values represent an average of a few instantaneous measurements within each ¼° × ¼° × daily bin. Clearly, there are biogeochemical processes (e.g., primary productivity, coastal upwelling) beyond the simple thermodynamic and carbonate chemistry controls driving this model that must contribute to some of the disparity between the ship and computed fields (Figure 5A). The model captures much of the longitudinal variation observed in the 1998 WOCE AR01 transect (Figure 5B) and the latitudinal trend visible in the 2003 WOCE A22 transect (Figure 5C).

3. Results

[20] Variations in temperature, alkalinity (primarily driven by salinity changes), and $pCO_{2,sw}$ impart important controls on aragonite saturation state (Ω_{arg}). The absolute change in Ω_{arg} per unit change in SST, A_T, and $pCO_{2,sw}$ within the domain of conditions encountered across the GCR (SST ± 10°C, A_T ± 200 μmol kg^{-1}, $pCO_{2,sw}$ ± 100 μatm) were derived using the CO2SYS program as:

$$\frac{d\Omega_{arg}}{dSST} = 0.117,\ \frac{d\Omega_{arg}}{dA_T} = 0.003,\ \frac{d\Omega_{arg}}{dpCO_{2,sw}} = -0.006. \quad (5)$$

[21] Thus seasonal variations in Ω_{arg} are dominated by thermodynamic effects but changes in carbonate chemistry should not be neglected. The combined effects produce a

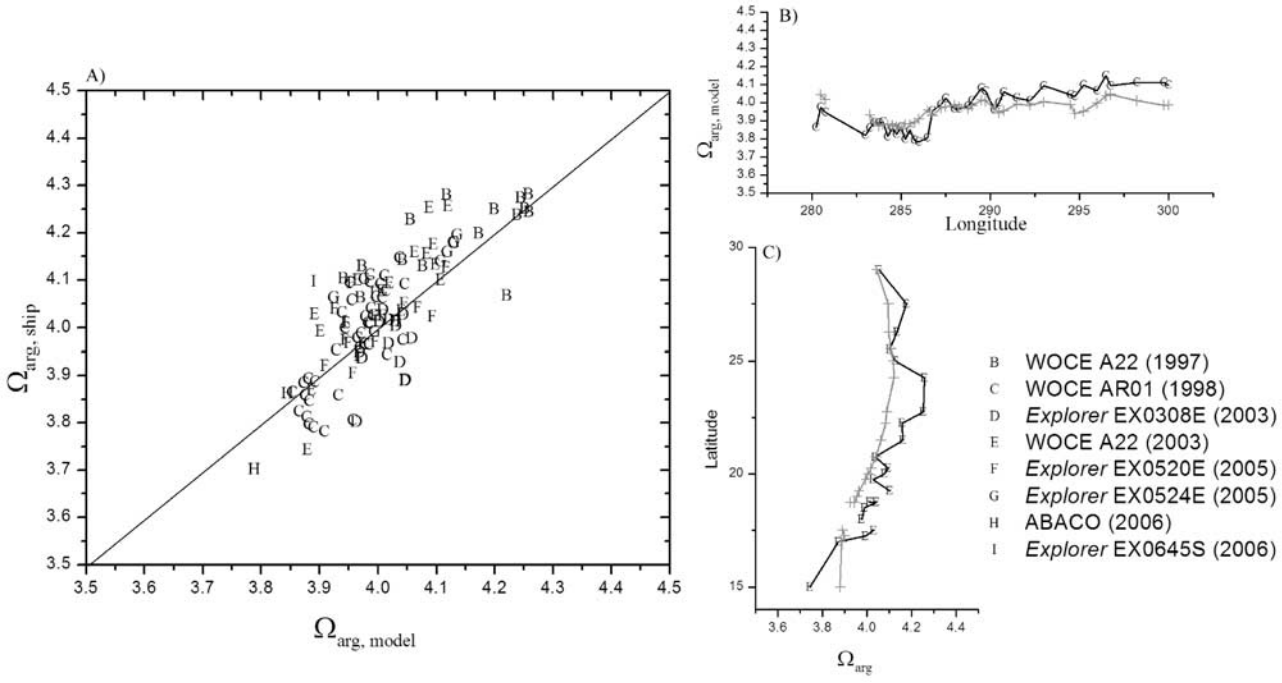

Figure 5. Comparison of bin-averaged ship versus collocated modeled Ω_{arg} values. Ship values were computed from measured carbonate chemistry data while modeled values were computed from $pCO_{2,sw}$ and A_T fields. (A) Values plot near the 1:1 line. (B and C) Ship values (black) compared with collocated modeled values (grey) as a function of longitude and latitude. The longitudinal track was obtained from the 1998 WOCE AR01 cruise transect while the latitudinal track is derived from the 2003 WOCE A22 transect.

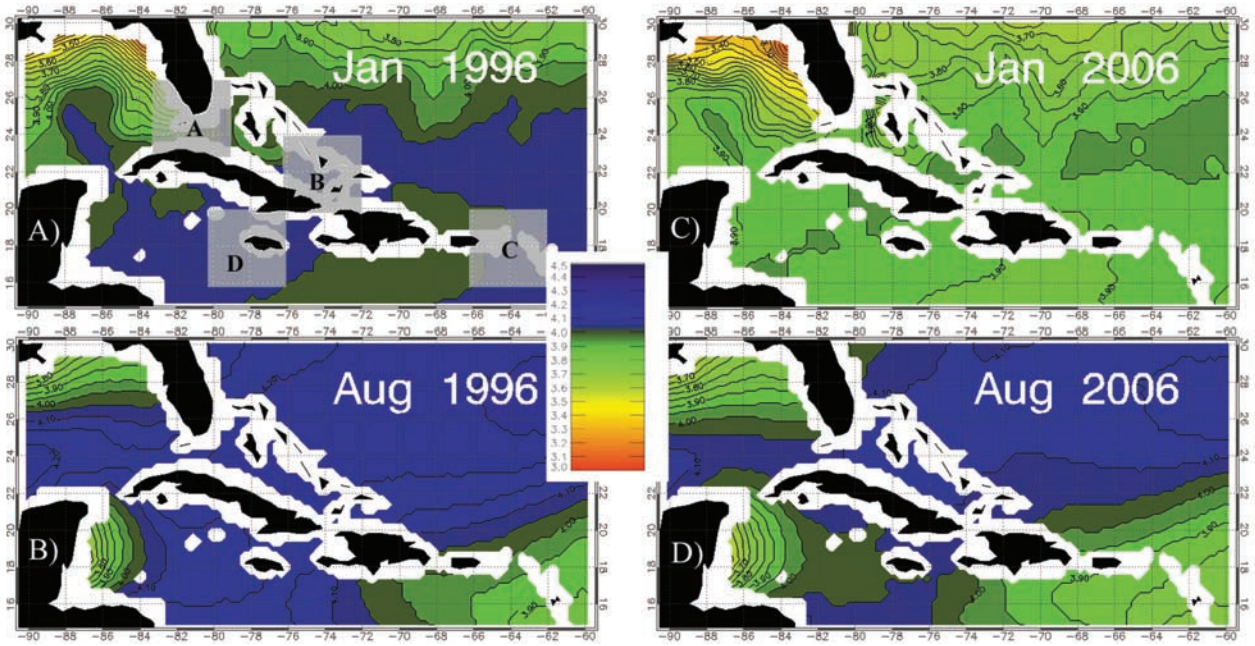

Figure 6. Seasonal variations in sea-surface aragonite saturation state (Ω_{arg}) in 1996 and 2006. Monthly mean values calculated for (A) January 1996, (B) August 1996, (C) January 2006, and (D) August 2006. Shaded areas denote regions from which trend calculations were performed (Figure 7).

dynamic and complex distribution in Ω_{arg} spatially and temporally across the GCR. The spatial variability in Ω_{arg} is typically close to 4% (δ = 0.15 Ω_{arg} units) in the wintertime with the lowest variability occurring in the spring and fall. During the wintertime, freshwater input from the Mississippi River plume appears to reduce Ω_{arg} in waters along the northwest coast of Florida to values 20% lower than the rest of the GCR (Figure 6). The highest and most stable Ω_{arg} values persist throughout the central GCR where the major carbonate platforms of the Bahamas and Greater Antilles occur. Regionally, the waters exhibit maximum values in August and September when, despite higher $pCO_{2,sw}$ values that drive down Ω_{arg}, the thermodynamic effect on carbonate equilibria is such that the increased SSTs yield elevated [CO_3^{2-}] in addition to a reduced carbonate mineral solubility thereby driving up Ω_{arg}. This summertime maximum is counteracted in the southeastern GCR because of low-salinity surface waters attributed to Orinoco River discharge. Seasonal trends of waters occupied by selected prominent reef systems illustrate the Florida Keys region likely experiences the greatest variability (Figure 7).

[22] For the GCR region, the decadal trends calculated using regression analysis of the annual computed mean $pCO_{2,sw}$ and Ω_{arg} are +2.2 μatm yr^{-1} (S.E. = 0.2, r^2 = 0.95, $P < 0.001$) and −0.012 Ω_{arg} yr^{-1} (S.E. = 0.001, r^2 = 0.97, $P < 0.001$) respectively. The model computes a regional decline in Ω_{arg} from 4.05 to 3.9 over the period 1996–2006 (Figure 8).

4. Discussion

[23] The secular change in GCR surface ocean carbonate chemistry in response to ocean acidification calculated in this study provides important independent support of other modeled rates previously reported. The model estimates the annual mean GCR surface ocean $pCO_{2,sw}$ increased 24 μatm, approximately that of the $pCO_{2,air}$, between 1996–2006 yielding a corresponding decrease in the carbonate ion of about 7 μmol kg^{-1} which agrees well with the assumed thermodynamic equilibrium calculations of *Broecker et al.* [1979] and the non-equilibrium model employed by *Orr et al.* [2005] for tropical waters. The model estimates an increase in dissolved inorganic carbon (DIC) at a rate of ~1.2 μmol kg^{-1} yr^{-1} in excellent agreement with the seasonally detrended rate of ~1.3 μmol mol kg^{-1} yr^{-1} observed at the Bermuda Atlantic Time-series (BATS) site between 1998 and 2006 [*Nelson et al.*, 2001]. The rate of decline in Ω_{arg} computed here is faster than that recently reported −0.007 ± 0.002 for the 22 year trend at BATS [*Bates*, 2007]. This difference may be related to a systematic increase in surface salinity of ~0.19 observed over at BATS during the 22 year period which would partially counteract the effects of ocean acidification by concentrating both A_T and Ca^{2+} and by reducing carbonate mineral solubility. No trend in surface salinity is apparent from the *Explorer of the Sea's* salinity data set and as this model is dependent on climatological salinity, no such increase would be reflected in the computed rates. Furthermore, the 22 year trend in $pCO_{2,atm}$ at BATS (+1.78 ± 0.02 μatm yr^{-1}) is slightly slower the rate computed from the Key Biscayne, Fl and Ragged Point, Barbados monitoring stations (+2.00 ± 0.04 μatm yr^{-1}). Finally, differences could reflect the length of time over which the regression is fit (22 year trend at BATS versus the 11 year trend computed in this study).

[24] On the basis of experimentally observed relationships between saturation state and coral community calcification rates, previous authors have assigned various categorical thresholds [*Guinotte et al.*, 2003; *Kleypas et al.*, 1999]. The following convention was employed by

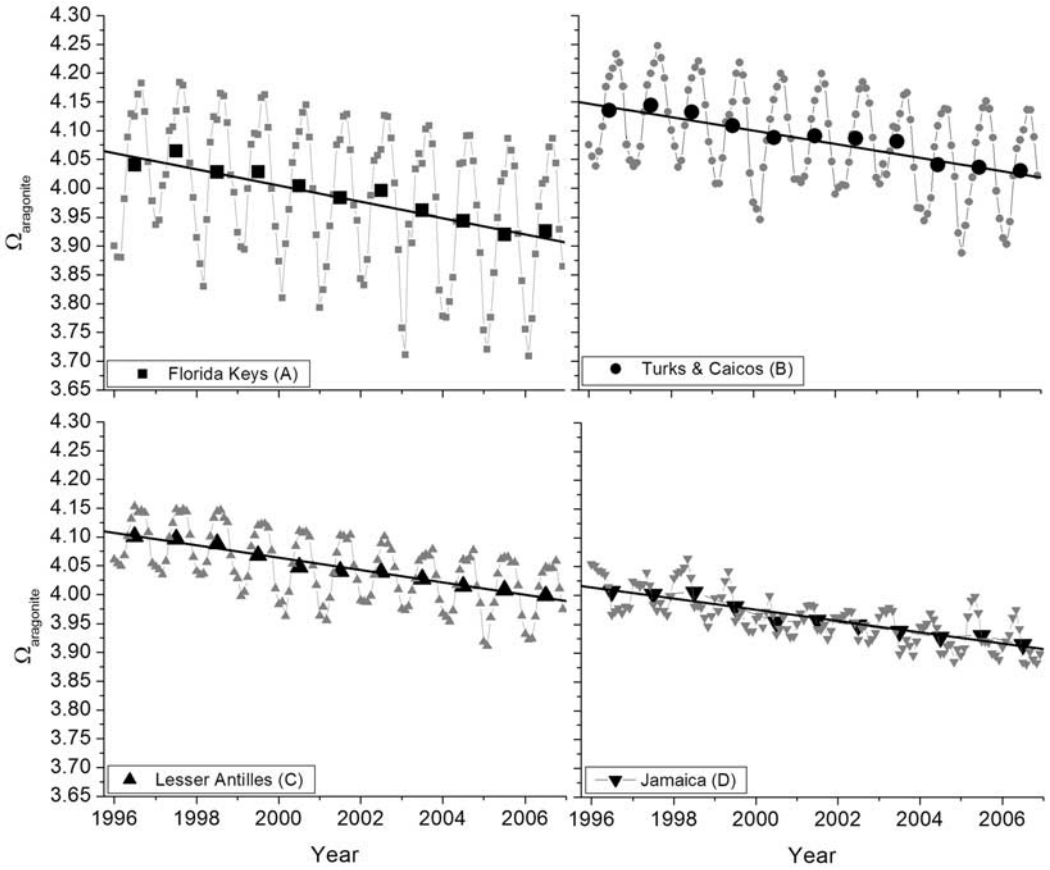

Figure 7. Trends in annual (black symbols) and monthly (grey symbols) mean sea-surface aragonite saturation state (Ω_{arg}) for the four regions occupied by prominent coral reefs denoted in Figure 6A. (A) Florida Keys. (B) Turks and Caicos. (C) Lesser Antilles. (D) Jamaica. Rates of change range from -0.014 ± 0.001 Ω_{arg} yr^{-1} for the Florida Keys region to 0.010 ± 0.001 Ω_{arg} yr^{-1} for the Jamaica region.

Guinotte et al. [2003]: surface waters exhibiting $\Omega_{arg} > 4$ are deemed "optimal", 3.5–4.0 are "adequate", 3.0–3.5 are "low", and <3.0 are considered "extremely marginal". It is thought that while calcification would persist in "extremely marginal" waters, the rates would likely not be sufficient to maintain net positive reef accretion thereby resulting in loss of reef structure. Certain reefs, especially those in naturally low Ω_{arg} waters such as the eastern Pacific, have been shown to move from net accretion to net erosion because of local environmental perturbations [*Eakin*, 1996, 2001; *Manzello et al.*, 2008]. Currently, the ranges of saturation state across the GCR generally reside within "adequate"-levels based on this scheme. However, under increasing $pCO_{2,air}$ concentrations, the annual GCR saturation state would fall to "low" levels when $pCO_{2,air}$ reaches approximately 450 μatm and become "extremely marginal" at concentrations above 550 μatm. Surface waters in the GCR would likely become undersaturated with respect to aragonite should $pCO_{2,atm}$ levels reach much beyond 900 μatm.

[25] Clearly illustrated by the computed monthly Ω_{arg} fields is that seasonal and spatial variability in carbonate chemistry may be of similar magnitude to the changes that have transpired over the past decade in the GCR. How the seasonal variability and long-term trend in carbonate chemistry is transposed onto the considerably higher variability experienced in the coastal waters occupied by coral reefs is not yet adequately characterized. Some models have suggested that the secular decline in saturation state for atolls and other semi-enclosed carbonate systems may strongly depend on mineral buffering reactions and water mass residence time [e.g., *Andersson et al.*, 2005]. At these semi-enclosed systems, calcification and respiration processes elevate $pCO_{2,sw}$ levels relative to offshore as documented in several studies [e.g., *Bates*, 2002; *Frankignoulle et al.*, 1994; *Gattuso et al.*, 1993, 1996, 1998a, 1998b, 1999; *Kawahata et al.*, 1997, 2000; *Kayanne et al.*, 1995, 2005; *Suzuki and Kawahata*, 1999, 2003, 2004; *Fagan and Mackenzie*, 2007]. As a consequence of the elevated $pCO_{2,sw}$ and the reduced alkalinity from calcification, saturation state can be appreciably lower on reefs relative to nearby oceanic waters. However, dissolution of high-Mg calcites could, at least initially, buffer these systems [*Morse et al.*, 2006]. Therefore efforts must be made to better refine the critical thresholds based on relationships between oceanic changes and corresponding changes in coastal systems.

[26] When concerns are raised with regards to the possible consequences of ocean acidification, the higher latitudes are typically highlighted as under the greatest threat since these waters already exhibit lower saturation states. Certainly there should be considerable concern that regions of

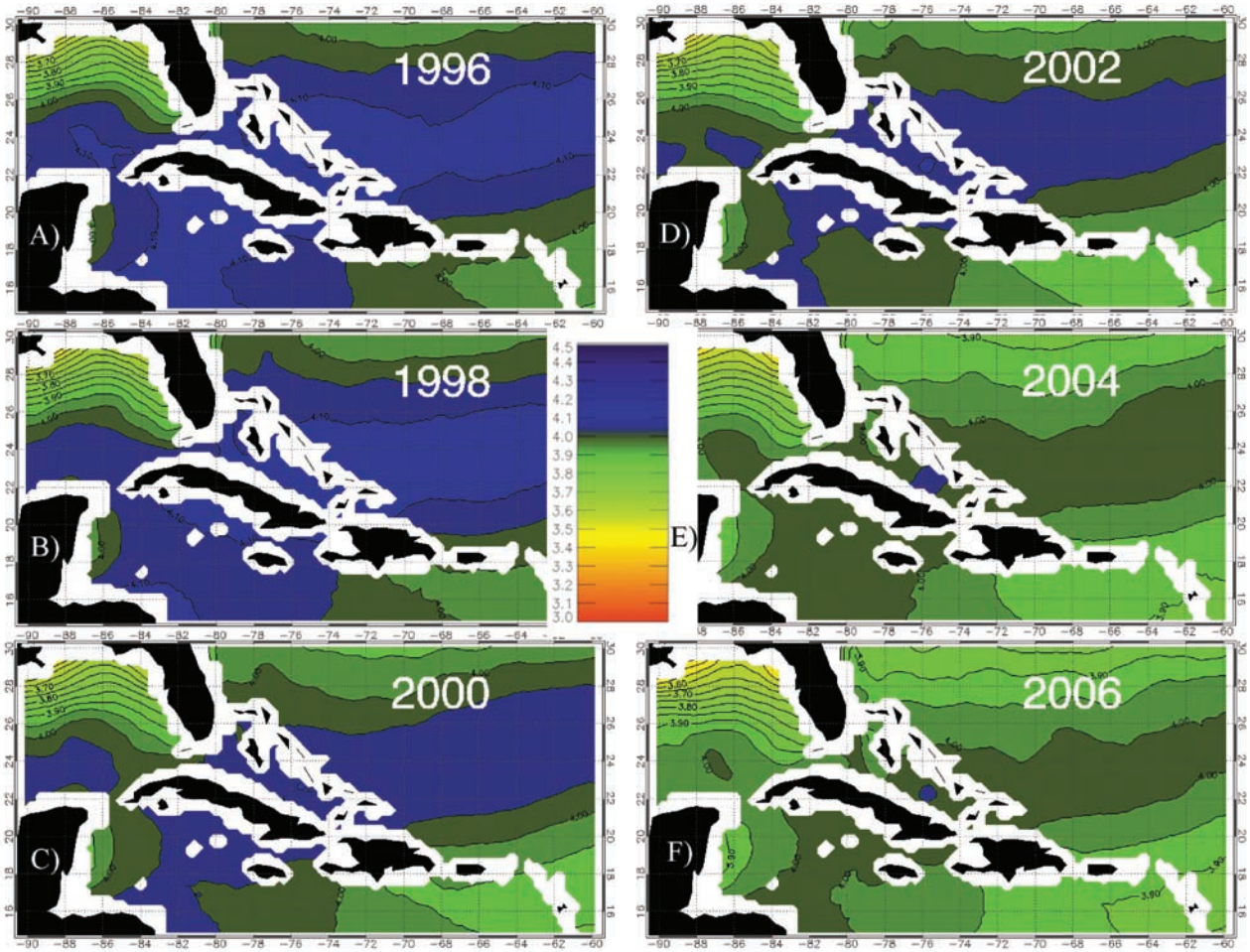

Figure 8. Secular decrease in sea-surface aragonite saturation state (Ω_{arg}) in the GCR as computed from the modeled fields of $pCO_{2,sw}$ and A_T. Calculated annual mean value in (A) 1996, (B) 1998, (C) 2000, (D) 2002, (E) 2004, and (F) 2006.

the Southern Ocean surface waters may become undersaturated with respect to aragonite by 2050 [*Orr et al.*, 2005]. However, since most studies to date demonstrate that the response in coral community calcification rate is not a step function, but instead roughly proportional to saturation state, it is likely that significant consequences may be unfolding in tropical waters as a result of the long-term decline in saturation state.

[27] We have provided an important application of satellite and modeled environmental data sets to upscale and extend *in situ* observations of carbonate chemistry permitting an examination of spatial and temporal variability not possible through ship observation alone. These new satellite-derived products can be produced on an operational basis to supplement *in situ* observations and provided at broader spatial and temporal scales than shipboard observations alone permit. As with any model, however, there are limitations and needed refinements. The climatological salinity fields offer perhaps the greatest limitation to the accuracy of this approach. Plans to incorporate modeled salinity fields or, in coming years, satellite acquired salinity fields such as those being planned for the NASA Aquarius mission could prove useful in improving our geochemical modeling capabilities. With increased availability and coverage of geochemical survey and time series data, this approach can be applied to map the seasonal distribution of saturation state in regions beyond the GCR.

5. Summary

[28] Here we extend observations obtained *in situ* from the Volunteer Observing Ship *Explorer of the Seas* and multiple geochemical surveys using satellite remote sensing and modeled environmental parameters to estimate the seasonal and spatial variability in Ω_{arg} and to evaluate the changes in surface ocean chemistry that have transpired over the past decade throughout the GCR. As numerous studies have now demonstrated a functional relationship between Ω_{arg} and coral community calcification, mapping its distribution seasonally can offer an important tool to the ocean acidification and coral reef research and management communities. The findings reveal the highest and most stable Ω_{arg} values persist throughout the central GCR where the carbonate platforms of the Bahamas and Greater Antilles occur. Summertime maximums in Ω_{arg} values occur in August and September when despite higher $pCO_{2,sw}$ values, the thermodynamic effect on carbonate equilibria drives up Ω_{arg}. Seasonal trends of waters occupied by selected prominent reef systems illustrate the Florida Key's region likely

experiences the greatest variability. While Ω_{arg} values across the GCR can be deemed "adequate" by current classification schemes, the annual mean Ω_{arg} for the GCR region has declined from 4.05 to 3.9 (±0.08) at a rate of −0.012 (S.E. = 0.001, $r^2 = 0.97$, $P < 0.001$) Ω_{arg} yr^{-1} from 1996 to 2006 as a consequence of rising atmospheric CO_2 and the resulting ocean acidification and may reach the "extremely marginal" levels ($\Omega_{arg} < 3.0$) should atmospheric CO_2 exceed 550 μatm.

[29] **Acknowledgments.** D.K.G. would like to acknowledge the continued support of the National Oceanic and Atmospheric Administration Coral Reef Conservation Program (NOAA CRCP) and the I.M. Systems Group. We would also like to recognize the contributions of the NOAA Global Monitoring Division (GMD) Carbon Cycle Cooperative Global Air Sampling Network and particularly the efforts of Thomas Conway. The observations on the Explorer of the Seas are funded by the Climate Observation Division of the NOAA Office of Oceanic and Atmospheric Research (OAR). F.J.M. would like to acknowledge the support of the Oceanographic Section of the National Science Foundation and National Oceanic and Atmospheric Association for supporting his CO_2 work. The manuscript contents are solely the opinions of the authors and do not constitute a statement of policy, decision, or position on behalf of NOAA or the U. S. Government.

References

Andersson, A. J., et al. (2005), Coastal ocean and carbonate systems in the high CO_2 world of the Anthropocene, *Am. J. Sci.*, *305*(9), 875–918.

Augustin, L., et al. (2004), Eight glacial cycles from an Antarctic ice core, *Nature*, *429*, 623–628.

Bacastow, R., and C. D. Keeling (1972), Atmospheric carbon dioxide and radiocarbon in the natural carbon cycle: II. Changes from A. D. 1700 to 2070 as deduced from a geochemical model, in *Carbon and the Biosphere; Proceedings of the 24th Brookhaven Symposium in Biology, Upton, N. Y., May 16–18, 1972*, edited by G. M. Woodwell and E. V. Pecan, pp. 86–135, Technical Information Center, U.S. Atomic Energy Commission, Washington, D. C.

Bates, N. R. (2002), Seasonal variability of the effect of coral reefs on seawater CO_2 and air-sea CO_2 exchange, *Limnol. Oceangr.*, *47*, 43–52.

Bates, N. R. (2007), Interannual variability of the oceanic CO_2 sink in the subtropical gyre of the North Atlantic Ocean over the last 2 decades, *J. Geophys. Res.*, *112*, C09013, doi:10.1029/2006JC003759.

Bates, N. R., A. F. Michaels, and A. H. Knap (1996), Seasonal and interannual variability of the oceanic carbon dioxide system at the U.S. JGOFS Bermuda Atlantic Time-series Site, *Deep Sea Res., Part II*, *43*, 347–383.

Bijma, J., B. Honisch, and R. E. Zeebe (2002), The impact of the ocean carbonate chemistry on living foraminiferal shell weight: Comment on "Carbonate ion concentration in glacial-age deep waters of the Caribbean Sea" by W. S. Broecker and E. Clark, *Geochem. Geophys. Geosyst.*, *3*(11), 1064, doi:10.1029/2002GC000388.

Borowitzka, M. A. (1981), Photosynthesis and calcification in the articulated coralline alga *Amphiroa anceps* and *A. foliaceae*, *Mar. Biol.*, *62*, 17–23.

Broecker, W. S., Y.-H. Li, and T.-H. Peng (1971), Carbon dioxide: Man's unseen artifact, in *Impingement of Man on the Oceans*, edited by D. W. Hood, pp. 287–324, Wiley Interscience, Hoboken, N. J.

Broecker, W. S., et al. (1979), Fate of fossil fuel carbon dioxide and the global carbon budget, *Science*, *206*, 409–418.

Burke, L., and J. Maidens (2004), *Reefs at Risk in the Caribbean*, 80 pp., World Resources Institute, Washington, D. C.

Caldeira, K., and M. E. Wickett (2003), Anthropogenic carbon and ocean pH, *Nature*, *425*(6956), 365.

Cooper, D. J., A. J. Watson, and R. D. Ling (1998), Variation of pCO_2 along a North Atlantic shipping route (U.K. to the Caribbean): A year of automated observations, *Mar. Chem.*, *60*, 147–164.

Dickson, A. G., and F. J. Millero (1987), A comparison of the equilibrium constants for the dissociation of carbonic acid in seawater media, *Deep Sea Res.*, *34*, 1733–1743.

Eakin, C. M. (1996), Where have all the carbonates gone? A model comparison of calcium carbonate budgets before and after the 1982–1983 El Niño, *Coral Reefs*, *15*, 109–119.

Eakin, C. M. (2001), A tale of two ENSO events: Carbonate budgets and the influence of two warming events and intervening variability, Uva Island, Panama, *Bull. Mar. Sci.*, *69*, 171–186.

Fagan, K. E., and F. T. Mackenzie (2007), Air-sea CO_2 exchange in a subtropical estuarine-coral reef system, Kaneohe Bay, Oahu, Hawaii, *Mar. Chem.*, *106*(1–2), 174–191.

Feely, R. A., R. Wanninkhof, H. B. Milburn, C. E. Cosca, M. Stapp, and P. P. Murphy (1998), A new automated underway system for making high precision pCO_2 measurements onboard research ships, *Anal. Chim. Acta*, *377*, 185–191.

Feely, R. A., C. L. Sabine, K. Lee, W. Berelson, J. Kleypas, V. J. Fabry, and F. J. Millero (2004), Impact of anthropogenic CO_2 on the $CaCO_3$ system in the oceans, *Science*, *305*, 362–366.

Frankignoulle, M., C. Canon, and J.-P. Gattuso (1994), Marine calcification as a source of carbon dioxide: Positive feedback of increasing atmospheric CO_2, *Limnol. Oceanogr.*, *39*, 458–462.

Gao, K., Y. Aruga, K. Asada, T. Ishihara, T. Akano, and M. Kiyohara (1993), Calcification in the articulated coralline alga *Corallina pilulifera*, with special reference to the effect of elevated CO_2 concentration, *Mar. Biol.*, *117*, 129–132.

Gattuso, J. P., M. Pichon, B. Delesalle, and M. Frankignoulle (1993), Community metabolism and air-sea CO_2 fluxes in a coral reef ecosystem (Morrea, French Polynesia), *Mar. Ecol. Prog. Ser.*, *96*, 259–267.

Gattuso, J. P., M. Frankignoulle, J. R. Ware, S. V. Smith, R. Wollast, W. R. Buddemeier, and H. Kayanne (1996), Coral reefs and carbon dioxide, *Science*, *271*, 1298–1300.

Gattuso, J. P., M. Frankignoulle, I. Bourge, S. Romaine, and R. W. Buddemeier (1998a), Effect of calcium carbonate saturation of seawater on coral calcification, *Global Planet. Change*, *18*, 37–46.

Gattuso, J. P., M. Frankignoulle, and R. Wollast (1998b), Carbon and carbonate metabolism in coastal aquatic ecosystems, *Annu. Rev. Ecol. Syst.*, *29*, 405–434.

Gattuso, J.-P., M. Frankignoulle, and S. V. Smith (1999), Measurement of community metabolism and significance in the coral reef CO_2 source-sink debate, *PNAS*, *96*, 13,017–13,022.

Goyet, C., N. Metzl, F. Millero, G. Eischeid, D. O'Sullivan, and A. Poisson (1998), Temporal variation of the sea surface CO_2/carbonate properties in the Arabian Sea, *Mar. Chem.*, *63*, 69–79.

Guinotte, J. M., R. W. Buddemeier, and J. A. Kleypas (2003), Future coral reef habitat marginality: Temporal and spatial effects of climate change in the Pacific basin, *Coral Reefs*, *22*(4), 551–558.

Karl, D. M., J. E. Dore, R. Lukas, A. F. Michaels, N. R. Bates, and A. H. Knap (2001), The U.S. JGOFS Time-series Observation Programs, *Oceanography*, *14*, 6–17.

Kawahata, H., A. Suzuki, and K. Goto (1997), Coral reef ecosystems as a source of atmospheric CO_2: Evidence from pCO_2 measurements of surface waters, *Coral Reefs*, *16*, 261–266.

Kawahata, H., A. Suzuki, T. Ayukai, and K. Goto (2000), Distribution of the fugacity of carbon dioxide in the surface seawater of the Great Barrier Reef, *Mar. Chem.*, *72*, 257.

Kayanne, H., A. Suzuki, and H. Saito (1995), Diurnal changes in the partial pressure of carbon dioxide in coral reef water, *Science*, *269*, 214–216.

Kayanne, H., H. Hata, S. Kudo, H. Yamano, A. Watanabe, Y. Ikeda, K. Nozaki, K. Kato, A. Negishi, and H. Saito (2005), Seasonal and bleaching-induced changes in coral reef metabolism and CO_2 flux, *Global Biogeochem. Cycles*, *19*, GB3015, doi:10.1029/2004GB002400.

Keeling, C. D., H. Brix, and N. Gruber (2004), Seasonal and long-term dynamics of the upper ocean carbon cycle at Station ALOHA near Hawaii, *Global Biogeochem. Cycles*, *18*, GB4006, doi:10.1029/2004GB002227.

Key, R. M., A. Kozyr, C. L. Sabine, K. Lee, R. Wanninkhof, J. L. Bullister, R. A. Feely, F. J. Millero, C. Mordy, and T. H. Peng (2004), A global ocean carbon climatology: Results from Global Data Analysis Project (GLODAP), *Global Biogeochem. Cycles*, *18*, GB4031, doi:10.1029/2004GB002247.

Kleypas, J. A., and C. M. Eakin (2006), Scientists' perceptions of threats to coral reefs: Results of a survey of coral reef researchers, *Bull. Mar. Sci.*, *80*, 419–436.

Kleypas, J. A., R. W. Buddemeier, D. Archer, J.-P. Gattuso, C. Langdon, and B. N. Opdyke (1999), Geochemical consequences of increased atmospheric carbon dioxide on coral reefs, *Science*, *284*(5411), 118–120.

Kuffner, I. B., et al. (2008), Decreased abundance of crustose coralline algae due to ocean acidification, *Nature Geosci.*, *1*(2), 114–117.

Langdon, C., and M. J. Atkinson (2005), Effect of elevated pCO_2 on photosynthesis and calcification of corals and interactions with seasonal change in temperature/irradiance and nutrient enrichment, *J. Geophys. Res.*, *110*, C09S07, doi:10.1029/2004JC002576.

Langdon, C., T. Takahashi, C. Sweeney, D. Chipman, and J. Goddard (2000), Effect of calcium carbonate saturation state on the calcification rate of an experimental coral reef, *Global Biogeochem. Cycles*, *14*, 639–654.

Langdon, C., W. S. Broecker, D. E. Hammond, E. Glenn, K. Fitzsimmons, S. G. Nelson, T.-H. Peng, I. Hajdas, and G. Bonani (2003), Effect of elevated CO_2 on the community metabolism of an experimental coral reef, *Global Biogeochem. Cycles*, *17*(1), 1011, doi:10.1029/2002GB001941.

Leclercq, N., J.-P. Gattuso, and J. Jaubert (2000), CO_2 partial pressure controls the calcification rate of a coral community, *Global Change Biol.*, *6*, 329–334.

Leclercq, N., J.-P. Gattuso, and J. Jaubert (2002), Primary production, respiration, and calcification of a coral reef mesocosm under increased CO_2 partial pressure, *Limnol. Oceanogr.*, *47*, 558–564.

Lee, K., L. T. Tong, F. J. Millero, C. L. Sabine, A. G. Dickson, C. Goyet, G.-H. Park, R. Wanninkhof, R. A. Feely, and R. M. Key (2006), Global relationships of total alkalinity with salinity and temperature in surface waters of the world's oceans, *Geophys. Res. Lett.*, *33*, L19605, doi:10.1029/2006GL027207.

Lewis, E., and D. W. R. Wallace (1998), Program Developed for CO_2 System Calculations. ORNL/CDIAC-105, Carbon Dioxide Information Analysis Center, Oak Ridge National Laboratory, U.S. Department of Energy, Oak Ridge, Tenn.

Manzello, D. P., et al. (2008), Poorly cemented coral reefs of the eastern tropical Pacific: Possible insights into reef development in a high-CO2 world, *Proceedings of the National Academy of Sciences of the United States of America*, *105*, 10,450–10,455.

Marshall, A. T., and P. Clode (2002), Effect of increased calcium concentration in sea water on calcification and photosynthesis in the scleractinian coral *Galaxea fascicularis*, *J. Exp. Biol.*, *205*, 2107–2113.

Marubini, F., H. Barnett, C. Langdon, and M. J. Atkinson (2001), Dependence of calcification on light and carbonate ion concentration for the hermatypic coral *Porites compressa*, *Mar. Ecol. Prog. Ser.*, *220*, 153–162.

Marubini, F., C. Ferrier-Pages, and J.-P. Cuif (2002), Suppression of growth in scleractinian corals by decreasing ambient carbonate ion concentration: A cross-family comparison, *Proc. R. Soc. London, Ser. B*, *270*, 179–184.

Mehrbach, C., C. H. Culberson, J. E. Hawley, and R. M. Pytkowicz (1973), Measurement of the apparent dissociation constants of carbonic acid in seawater at atmospheric pressure, *Limnol. Oceanogr.*, *18*, 897–907.

Monterey, G. I., and S. Levitus (1997), Climatological cycle of mixed layer depth in the world ocean, 5 pp., U.S. Gov. Printing Office, NOAA NESDIS, Washington, D.C.

Morse, J. W., and R. A. Berner (1972), Dissolution kinetics of calcium-carbonate in sea-water: 2. Kinetic origin for lysocline, *Am. J. Sci.*, *272*(9), 840–851.

Morse, J. W., D. K. Gledhill, and F. J. Millero (2003), $CaCO_3$ precipitation kinetics in waters from the great Bahama bank: Implications for the relationship between bank hydrochemistry and whitings, *Geochim. Cosmochim. Acta*, *67*, 2819–2826.

Morse, J. W., et al. (2006), Initial responses of carbonate-rich shelf sediments to rising atmospheric pCO(2) and "ocean acidification": Role of high Mg-calcites, *Geochim. Cosmochim. Acta*, *70*(23), 5814–5830.

Nelson, N. B., N. R. Bates, D. A. Siegel, and A. F. Michaels (2001), Spatial variability of the CO_2 sink in the Sargasso Sea, *Deep Sea Res., Part II*, *48*, 1801–1821.

Ohde, S., and M. M. Hossain (2004), Effect of $CaCO_3$ (aragonite) saturation state of seawater on calcification of *Porites* coral, *Geochem. J.*, *38*, 613–621.

Olsen, A., J. A. Trinanes, and R. Wanninkhof (2004), Sea-air flux of CO_2 in the Caribbean Sea estimated using in situ and remote sensing data, *Remote Sens. Environ.*, *89*, 309–325.

Orr, J. C., et al. (2005), Anthropogenic ocean acidification over the twenty-first century and its impact on calcifying organisms, *Nature*, *437*, 681–686.

Petit, J. R., et al. (1999), Climate and atmospheric history of the past 420,000 years from the Vostok ice core, Antarctica, *Nature*, *399*, 429–436.

Reynaud, S., N. Leclercq, S. Romaine-Lioud, C. Ferrier-Pages, J. Jaubert, and J.-P. Gattuso (2003), Interacting effects of CO_2 partial pressure and temperature on photosynthesis and calcification in a scleractinian coral, *Global Change Biol.*, *9*, 1660–1668.

Reynolds, R. W., T. M. Smith, C. Liu, D. B. Chelton, K. S. Casey, and M. G. Schlax (2007), Daily high-resolution blended analyses, *J. Clim.*, *20*, 5473–5496.

Riebesell, U. (2004), Effects of CO_2 enrichment on marine phytoplankton, *J. Oceanogr.*, *60*, 719–729.

Riebesell, U., I. Zondervan, B. Rost, P. D. Tortell, R. E. Zeebe, and F. M. M. Morel (2000), Reduced calcification of marine plankton in response to increased atmospheric CO_2, *Nature*, *407*, 364–367.

Sabine, C. L., et al. (2004), The oceanic sink for anthropogenic CO_2, *Science*, *305*, 367–371.

Siegenthaler, U., et al. (2005), Stable carbon cycle-climate relationship during the late Pleistocene, *Science*, *310*, 1313–1317.

Suzuki, A., and H. Kawahata (1999), Partial pressure of carbon dioxide in coral reef lagoon, *J. Oceanogr.*, *55*, 731–745.

Suzuki, A., and H. Kawahata (2003), Carbon budget of coral reef systems: An overview of observations in fringing reefs, barrier reefs and atolls in the Indo-Pacific regions, *Tellus*, *55B*, 428–444.

Suzuki, A., and H. Kawahata (2004), Reef water CO_2 system and carbon production of coral reefs: Topographic control of system-level performance, in *Global Environmental Change in the Ocean and on Land*, edited by H. K. M. Shiyomi et al., pp. 229–248, TERRAPUB, Tokyo.

Takahashi, T., K. Olafsson, J. G. Goddard, D. W. Chipman, and S. C. Sutherland (1993), Seasonal variation of CO_2 and nutrients in the high-latitude surface oceans: A comparative study, *Global Biogeochem. Cycles*, *7*, 843–878.

Thoning, K. W., T. J. Conway, N. Zhang, and D. Kitzis (1995), Analysis system for measurement of CO_2 mixing ratios in flask air samples, *J. Atmos. Oceanic Tech.*, *12*, 1349–1356.

Wanninkhof, R., and K. Thoning (1993), Measurement of fugacity of CO_2 in surface water using continuous and discrete sampling methods, *Mar. Chem.*, *44*(2–4), 189.

Wanninkhof, R., A. Olsen, and J. Trinanes (2007), Air-sea CO_2 fluxes in the Caribbean Sea from 2002–2004, *J. Mar. Syst.*, *66*, 272–284.

Weiss, R. F. (1974), Carbon dioxide in water and seawater: The solubility of a non-ideal gas, *Mar. Chem.*, *2*, 203–215.

Yang, C. P., et al. (2003), Origin, Ver. 7.5, OriginLab Corporation, Northhampton, Mass.

Yates, K. K., and R. B. Halley (2006), CO_3^{2-} concentration and pCO_2 thresholds for calcification and dissolution on the Molokai reef flat, Hawaii, *Biogeosciences*, *3*, 1–13.

M. Eakin and D. K. Gledhill, NOAA NESDIS Coral Reef Watch, E/RA31, 1335 East-West Highway, Silver Spring, MD 20910-3226, USA. (dwight.gledhill@noaa.gov)

F. J. Millero, Rosenstiel School, University of Miami, 4600 Rickenbacker Causeway, Miami, FL 33149, USA. (f.millero@rsmas.miami.edu)

R. Wanninkhof, NOAA OAR AOML, 4301 Rickenbacker Causeway, Miami, FL 33149, USA.